View metadata, citation and similar papers at core.ac.uk
brought to you by CORE
provided by Diposit Digital de Documents de la UAB

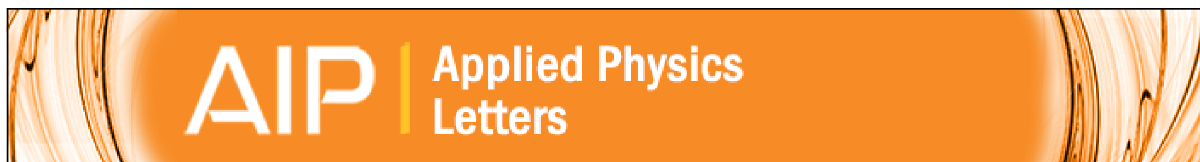


# Mesoscopic approach to the soft breakdown failure mode in ultrathin SiO 2 films

Enrique Miranda and Jordi Suñé

Citation: Applied Physics Letters **78**, 225 (2001); doi: 10.1063/1.1339259
View online: http://dx.doi.org/10.1063/1.1339259
View Table of Contents: http://scitation.aip.org/content/aip/journal/apl/78/2?ver=pdfcov
Published by the AIP Publishing

Instruments for advanced science

Gas Analysis

- dynamic measurement of reaction gas streams
- catalysis and thermal analysis
- molecular beam studies
- dissolved species probes
- fermentation, environmental and ecological studies

Surface Science

- UHV TPD
- SIMS
- end point detection in ion beam etch
- elemental imaging - surface mapping

Plasma Diagnostics

- plasma source characterization
- etch and deposition process reaction kinetic studies
- analysis of neutral and radical species

Vacuum Analysis

- partial pressure measurement and control of process gases
- reactive sputter process control
- vacuum diagnostics
- vacuum coating process monitoring

contact Hiden Analytical for further details
HIDEN ANALYTICAL
info@hideninc.com

www.HidenAnalytical.com
CLICK to view our product catalogue

This article is copyrighted as indicated in the article. Reuse of AIP content is subject to the terms at: http://scitation.aip.org/termsconditions. Downloaded to IP: 158.109.223.71 On: Wed, 26 Feb 2014 09:54:57

APPLIED PHYSICS LETTERS VOLUME 78, NUMBER 2 8 JANUARY 2001

# Mesoscopic approach to the soft breakdown failure mode in ultrathin $SiO_2$ films

Enrique Miranda[a)]
*Laboratorio de Física de Dispositivos-Microelectrónica, Facultad de Ingeniería, Universidad de Buenos Aires, Paseo Colón 850, 1063 Buenos Aires, Argentina*

Jordi Suñé
*Departament d'Enginyeria Electrònica, Universitat Autònoma de Barcelona, 08193-Bellaterra, Spain*

(Received 1 June 2000; accepted for publication 16 November 2000)

We present an analytic model for the soft breakdown failure mode in ultrathin $SiO_2$ films based on the conduction theory through quantum point contacts. The breakdown path across the oxide is represented by a three-dimensional constriction in which, due to the lateral confinement of the electron wave functions, discrete transverse energy levels arise. In the longitudinal direction, such levels are viewed by the incoming electrons as effective potential barriers, which can be treated using the one-dimensional tunneling formalism. In addition, it is shown that our mesoscopic approach is also consistent with the hard breakdown conduction mode. © *2001 American Institute of Physics.* [DOI: 10.1063/1.1339259]

Since the discovery of conductance quantization in 1988 by van Wees *et al.*[1] and by Wharam *et al.*,[2] electron transport in narrow constrictions has been extensively investigated. The phenomenon, which is nothing but the manifestation of the wave-like character of electrons when laterally confined, has been observed in a wide variety of experimental setups as well as under very different measurement conditions: split gate devices,[1,2] mechanically controllable break junctions,[3] scanning tunneling microscopes,[4] amorphous-silicon memory structures,[5] gold coated relay contacts,[6] etc. This seeming universal behavior of electrons when passing through atom-sized volumes points out that, in a general sense, the conducting properties of such systems are neither essentially linked to the origin nor to the particular microscopic nature of the path connecting the electrodes. Only their dimensions, with the consequent current and energy funneling effects,[7] seem to be relevant. Moreover, experimental conditions *a priori* quite far from those expected for the phenomenon to be observable do not limit its detection: conductance quantization has been reported both at high applied bias[5,6] and at room temperature.[8,9]

Here, we show that the postbreakdown conduction in $SiO_2$ films can also be explained by means of concepts developed to deal with the transport problem in mesoscopic systems. Phenomenally, the dielectric breakdown of an oxide is characterized by an abrupt loss of its insulating capability, which is electrically related to the appearance of a local low resistance path running between the electrodes. In this regard, there is wide agreement in ascribing the origin of this path to the generation of defects caused by the application of a previous electrical wear-out condition.[10] Two remarkably dissimilar breakdown modes have been detected in ultrathin oxides: the so-called soft or quasibreakdown (SBD) and the hard or catastrophic breakdown (HBD) modes; their names being related to the severity of the event. Our proposal is that the SBD's and HBD's particular features essentially arise as a consequence of the lateral dimensions of the breakdown spots. In this context, and as considered in a previous work,[11] we will identify the breakdown path with a three-dimensional (3D) constriction and the semiconductor electrodes with infinite charge reservoirs attached at its two ends. This is the picture usually considered in the analysis of mesoscopic conducting devices,[12] which will be further adapted to represent the system under study.

The measurements were performed at room temperature on conventional metal–oxide–semiconductor (MOS) capacitors with oxide thicknesses of 3 and 4.6 nm and areas of about $10^{-5}\,cm^2$. Following standard microelectronic techniques, the oxides were thermally grown onto an $n$-type ($\sim 10^{15}\,cm^{-3}$) silicon substrate at 800 °C. The top electrode was an $n^+$-polysilicon ($\sim 10^{18}\,cm^{-3}$) gate. As is well known, the application of a proper constant voltage or current stress, or even a voltage sweep, can lead to the appearance of SBD or HBD indistinctly. Typical SBD and HBD current–voltage ($I-V$) curves as well as the Fowler–Nordheim (FN) conduction characteristic, the latter measured prior to the breakdown event, are illustrated in Fig. 1.

Following previous approaches,[13,14] the schematic energy diagram of a narrow constriction with a large applied bias is depicted in Fig. 2. We consider that the total applied voltage ($V$) partly drops in the semiconductor electrodes ($V_0$) and partly at the two edges of the conduction path ($V_c$), i.e., $V=V_c+V_0$. Although $V_0$ is expected to be a function of the applied bias, in order not to introduce additional complexities, we will take it as a constant representing an average potential drop. In addition, a parameter $\beta$ controls the fraction of the potential $V_c$ that drops abruptly on the source side of the constriction. In the zero-temperature limit, the current through a potential barrier is[15]

$$I=\frac{2e}{h}\int_{E_F-(1-\beta)eV_c}^{E_F+\beta eV_c} T(E,V_c)\,dE, \tag{1}$$

[a)]Electronic mail: emirand@tron.fi.uba.ar

This article is copyrighted as indicated in the article. Reuse of AIP content is subject to the terms at: http://scitation.aip.org/termsconditions. Downloaded to IP: 158.109.223.71 On: Wed, 26 Feb 2014 09:54:57

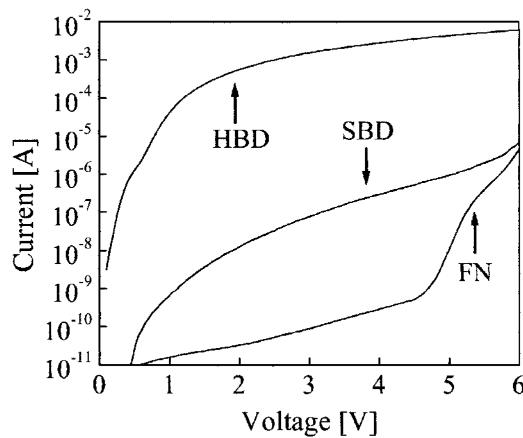


FIG. 1. Typical breakdown modes of an ultrathin oxide in a MOS structure. FN refers to the Fowler–Nordheim $I-V$ characteristic measured on the fresh sample, SBD to soft breakdown, and HBD to hard breakdown.

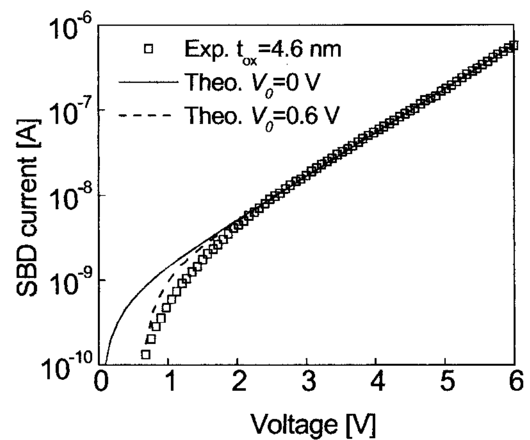


FIG. 3. Experimental and theoretical $I-V$ characteristics associated with the soft breakdown conduction mode. $V_0$ is a parameter of the model and represents an average potential drop in the electrodes.

where $e$ is the electron charge, $h$ Planck's constant, $E$ the electron energy, $E_F$ the Fermi level, and $T$ the transmission probability. By decoupling the Schrödinger equation in transverse and longitudinal equations, the conduction problem through a 3D constriction can be straightforwardly treated as a one-dimensional (1D) tunneling problem.[16] When the lateral confining potential is narrow, a discrete set of transverse energy levels, $E_n(z)$, arises along the constriction. As in a quantum well, tighter confinement rises such levels, each of them acting as a longitudinal potential barrier for the incoming electrons. If the modes $E_n(z)$ are expanded to second order in $z$ in the vicinity of the constriction's bottleneck (arbitrarily located at $z=0$), the transmission probability is[15,16]

$$T(E)=\sum_{n=1}^{N}\{1+\exp[-\alpha_n(E-E_n)]\}^{-1}, \qquad (2)$$

where $N$ is the number of available conducting channels, and $E_n=E_n(0)$ and $\alpha_n$ are constants dependent on the geometry of the constriction and the electron effective mass. Hereafter, we will assume that levels $E_n$ are not affected by the sample bias, that the effective cross-sectional area at the narrowest part of the constriction is independent of the electron energy (as in a box-type potential well), and that the potential drops symmetrically at the two ends of the constriction ($\beta=1/2$). Consider now that $E \ll E_1$, i.e., the electron energy is well below the bottom of the first subband level, as depicted in Fig. 2. Under these assumptions, using Eqs. (1) and (2), the current is.

$$I=\frac{4e}{\alpha_1 h}\exp[-\alpha_1(E_1-E_F)]\sinh\left(\frac{\alpha_1 e(V-V_0)}{2}\right). \qquad (3)$$

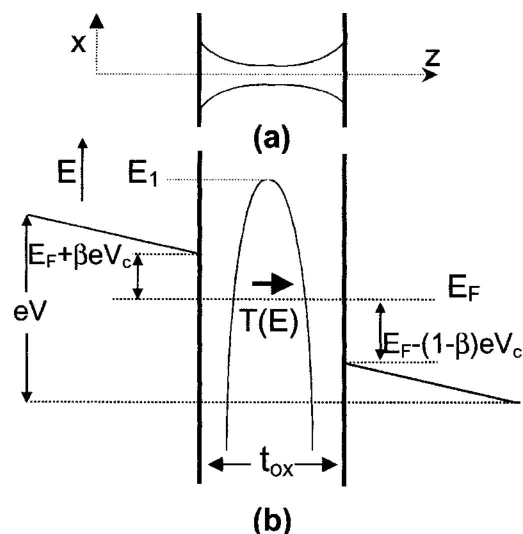


FIG. 2. (a) Top view of the constriction (breakdown path) between the electrodes. (b) Energy diagram of the constriction shown in (a) with a large applied bias. $E_1$ is the bottom of the first energy subband, $V$ is the applied voltage, $V_c$ the potential drop across the constriction, and $t_{ox}$ the oxide thickness. $E_F$ is the Fermi level and $\beta$ is a parameter of the model. $T(E)$ is the transmission probability for the inverted parabolic barrier.

Figure 3 shows, for comparison, two fittings to a typical SBD $I-V$ characteristic using Eq. (3), one with $V_0=0$ V and the other with $V_0=0.6$ V. Considering the latter value, the fitting yields $\alpha_1 \approx 2.38\,\mathrm{eV}^{-1}$ and an effective potential barrier height of $E_1-E_F \approx 4.41$ eV, which is a very reasonable result [other tunneling models report barrier heights of 6.2 (Ref. 17) and 4.2 eV (Ref. 18)]. It is worth emphasizing that this barrier is not material related like that of the Si–$SiO_2$ interface, for example. Physically, it arises as a consequence of the fact that the electrons' transversal wavelength associated with the energy window of the current-carrying states is larger than the effective diameter of the narrowest point along the SBD path.

On the other hand, when $E \gg E_N$, i.e., when the energy of the incoming electrons is higher than the bottom of the energy subband $N$, Eqs. (1) and (2) yield $T(E) \approx N$ and $G(V)=dI/dV \approx NG_0$, $G_0=2e^2/h$ being the quantum conductance unit. In this connection, Fig. 4 shows several conductance–voltage ($G-V$) characteristics measured after the detection of successive HBD events on the same sample. The events were induced by high-field voltage sweeps as reported in Ref. 19. The lower trace in Fig. 4 corresponds to the foremost open HBD spot and has a conductance plateau at approximately $G \approx 2G_0$. The second curve corresponds to the currents flowing in parallel through the first and second induced spots. Therefore, the conductance of this second spot is about $2G_0$ as well. The differences between successive $G-V$ curves clearly reveal that there are spots with conductances of about 1, 2, and 3 $G_0$, as predicted by our

This article is copyrighted as indicated in the article. Reuse of AIP content is subject to the terms at: http://scitation.aip.org/termsconditions. Downloaded to IP: 158.109.223.71 On: Wed, 26 Feb 2014 09:54:57

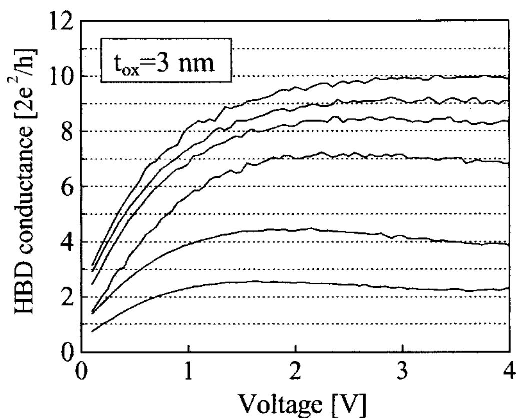


FIG. 4. Successive experimental low-field hard breakdown $G-V$ characteristics measured on the same sample.

model. Notice that, at lower bias, all the curves are affected by the potential drops in the electrodes. The simulation of this effect in the differential characteristics would require detailed knowledge of $V_0(V)$, which is still unavailable.

In the last few years, several models have been proposed to explain SBD. They are based on a wide variety of mechanisms such as direct tunnel through a local thinned down oxide,[20] variable range hopping,[21] percolation in nonlinear conductor networks,[18] inelastic quantum tunneling,[22] and quantum wires with resonant tunneling.[23] Although the results predicted by all these models are in partial agreement with the experimental SBD data, none of them, except that of Ting,[23] has been extrapolated to the HBD limit. However, in Ting's model, a coverage of 10% of the device area with quantum wires is necessary in order to reach the experimental current level of both SBD and HBD. This is clearly at variance with the area of $10^{-14}-10^{-12}\,\text{cm}^2$ attributed to the breakdown spots.[10,24] In addition, although a thorough analysis of the referred models is out of the scope of this letter, let us mention that in our approach the oxide thickness value does not enter into the description of the phenomenon. In this regard, we have recently shown that the SBD $I-V$ characteristics are essentially independent of this parameter for oxides of 3, 4.2, and 4.9 nm thick.[25] This is clear proof of the local character of the blocking mechanism governing the current in the case of SBD being the features of the electrostatic potential at the bottleneck of the conducting path.

In conclusion, we have presented an analytic model for the soft breakdown current in ultrathin $SiO_2$ films based on the physics of mesoscopic conducting devices. The transmission properties of narrow constrictions have been invoked to explain the difference between the conduction modes referred to as soft and hard breakdown. It was proposed that the lateral dimensions of the breakdown spot determine whether electron transport is dominated by tunneling through an area-related potential barrier (soft) or by ballistic point contact conduction (hard).

The authors acknowledge the partial support of the Dirección General de Enseñanza Superior (DGES) under Project No. PB97-0182, the UBACyT program under Project No. JI04, and the Fundación Antorchas.


[1] B. van Wees, H. van Houten, C. Beenakker, J. Williamson, L. Kouwenhouven, D. van der Marel, and C. Foxon, Phys. Rev. B **60**, 848 (1988).
[2] D. Wharam, T. Thornton, R. Newbury, M. Pepper, H. Ahmed, J. Frost, D. Hasko, D. Peacock, D. Ritchie, and G. Jones, J. Phys. C **21**, L209 (1988).
[3] J. Krans, J. van Ruitenbeek, V. Fisun, I. Yanson, and L. De Jongh, Nature (London) **375**, 767 (1995).
[4] H. Ohnishi, Y. Kondo, and K. Takayanagi, Nature (London) **395**, 780 (1998).
[5] J. Hajto, A. Owen, S. Gage, A. Snell, P. LeComber, and M. Rose, Phys. Rev. Lett. **66**, 1918 (1991).
[6] H. Yasuda and A. Sakai, Phys. Rev. B **56**, 1069 (1997).
[7] R. Landauer, Phys. B-Cond. Matt. **68**, 217 (1987).
[8] J. Pascual, J. Méndez, J. Gómez-Herrero, A. Baró, N. Garcia, and V. Thien Binh, Phys. Rev. Lett. **71**, 1852 (1993).
[9] L. Olesen, E. Lægsgsgaard, I. Stensgaard, F. Besenbacher, J. Schiøtz, P. Stoltze, K. Jacobsen, and J. Nørskov, Phys. Rev. Lett. **72**, 2251 (1994).
[10] J. Stathis, J. Appl. Phys. **86**, 5757 (1999).
[11] J. Suñé, E. Miranda, M. Nafría, and X. Aymerich, Appl. Phys. Lett. **75**, 959 (1999).
[12] S. Datta, *Electronic Transport in Mesoscopic Systems* (Cambridge, University Press, New York, 1997).
[13] H. Xu, Phys. Rev. B **47**, 15630 (1993).
[14] J. Pascual, J. Torres, and J. Sáenz, Phys. Rev. B **55**, R16029 (1997).
[15] T. Ouchterlony and K. Berggren, Phys. Rev. B **52**, 16329 (1995).
[16] M. Brandbyge, J. Schiøtz, M. Sørensen, P. Stoltze, K. Jacobser, J. Nørskov, L. Olesen, E. Lægsgaard, I. Stensgaard, and F. Besenbacher, Phys. Rev. B **52**, 8499 (1995).
[17] O. Halimaoui, O. Brieré, and G. Ghibaudo, Microelectron. Eng. **36**, 157 (1997).
[18] M. Houssa, T. Nigam, P. Mertens, and M. Heyns, J. Appl. Phys. **84**, 4351 (1998).
[19] E. Miranda, J. Suñé, R. Rodríguez, M. Nafría, and X. Aymerich, Microelectron. Eng. **48**, 171 (1999).
[20] T. Yoshida, S. Miyazaki, and M. Hirose, *Extended Abstracts of the 1996 International Conference on Solid State Devices and Materials* (Business Center for Academic Societies, Japan, Tokyo, 1996), p. 539.
[21] K. Okada and K. Taniguchi, Appl. Phys. Lett. **70**, 351 (1997).
[22] T. Nigam, Ph.D. thesis, Katholieke Universiteit Leuven, Leuven, Belgium, 1999, p. 64.
[23] D. Ting, Appl. Phys. Lett. **74**, 585 (1999).
[24] R. Degraeve, G. Groseneken, R. Bellens, J. Ogier, M. Depas, J. Roussel, and H. Maes, IEEE Trans. Electron Devices **45**, 904 (1998).
[25] E. Miranda, J. Suñé, R. Rodríguez, M. Nafría, X. Aymerich, L. Fonseca, and F. Campabadal, IEEE Trans. Electron Devices **47**, 82 (2000).


This article is copyrighted as indicated in the article. Reuse of AIP content is subject to the terms at: http://scitation.aip.org/termsconditions. Downloaded to IP: 158.109.223.71 On: Wed, 26 Feb 2014 09:54:57